Precise determination of the dipole matrix element and radiative lifetime of the ^{39}K $4p$ state by photoassociative spectroscopy

H. Wang,[1] J. Li,[1] X. T. Wang,[1] C. J. Williams,[2,*] P. L. Gould,[1] and W. C. Stwalley[1]

[1]*Department of Physics, U-46, University of Connecticut, Storrs, Connecticut 06269*
[2]*Atomic Physics Division, National Institute of Standards and Technology, Gaithersburg, Maryland 20899*

Rovibrational levels ($v=0$–30) of the 0_g^- ''pure long-range'' state of ^{39}K$_2$ are observed by photoassociative spectroscopy of ultracold potassium atoms prepared in a high-density magneto-optical trap. The measured molecular binding energies are used to precisely determine the long-range dipole-dipole potential constant C_3^Π of the $K(4s)+K(4p)$ asymptote and the radiative lifetime of the $4p$ state. We determine $C_3^\Pi=-5.456(9)$ zJ nm^3 ($-8.445(14)$ a.u.), $\tau(4\,^2P_{3/2})=26.34(5)$ ns, and $\tau(4\,^2P_{1/2})=26.69(5)$ ns. Our result is a significant improvement in precision over previous lifetime measurements and agrees well with the recent fast-beam experiment [U. Volz and H. Schmoranzer, Phys. Scr. **T65**, 48 (1996)]. [S1050-2947(97)50603-2]

PACS number(s): 32.70.Cs, 32.80.Pj, 34.20.Cf, 34.50.Rk

Accurate measurements of radiative lifetimes of alkali-metal atoms constitute important tests of atomic theories. The reliability of these theories is crucial in the interpretation of fundamental measurements involving atoms, e.g., parity nonconservation measurements in Cs [1]. Long-standing discrepancies between experiment and theory for the Li $2p$ and Na $3p$ radiative lifetimes were recently resolved by high-precision measurements [2–6]. As an alternative to conventional direct (e.g., fast-beam [4]) lifetime measurements, the recently developed photoassociative spectroscopy of ultracold atoms [7,8] has proven to be a powerful technique for determination of radiative lifetimes with uncertainties $\sim0.1\%$ [2–3,6]. Such radiative lifetimes of the first excited state of alkali-metal atoms [2–3,6,9] are based on the equation, $\tau=-(3\hbar/4C_3^\Pi)(\lambda/2\pi)^3$, where τ is the radiative lifetime, $C_3^\Pi=-|\langle s|z|p\rangle|^2$ the long-range resonant dipole-dipole potential constant, and λ the transition wavelength. Since C_3 can be derived from the binding energies of the long-range molecular vibrational levels, very small relative uncertainties can be achieved (0.03% for Li [3], 0.1% for Na [6], and 0.2% here for K).

The radiative lifetime of the K $4p$ state is much less accurately determined than the corresponding Li and Na lifetimes. There have been five previous experimental measurements for $4\,^2P_{3/2}$ [10–14] and three recent theoretical calculations [15–17]. Uncertainties in the experimental results range from 1.9% to 3.4%, making them consistent with each other (3.4% standard deviation) and with the theory. A recent fast-beam measurement [18] (quoted uncertainty of 0.26%) has significantly improved the experimental situation. However, this value deviates from the theoretical results by -2.7, $+5.1$, and -2.1 of its standard deviations (-0.72%, $+1.4\%$, and -0.57%, respectively). Our spectroscopic lifetime determination, with completely different systematic uncertainties, agrees quite well (within the combined uncertainties) with the fast-beam result, reinforcing the mar-

ginal agreement with existing theoretical predictions. The situation for the $4\,^2P_{1/2}$ lifetime is similar.

''Pure long-range'' molecules, first proposed by Stwalley, Uang, and Pichler in 1978 [19–23], are special molecular electronic states where all vibrational levels have both inner and outer classical turning points at very large internuclear distances. In particular, the 0_g^- state of K$_2$ has a potential well depth of 6.495 cm^{-1} and an equilibrium distance $R_e=2.76$ nm as determined here. The entire potential well has negligible chemical exchange contributions since it is outside $R_{\text{LR-}m}$ (1.62 nm for K$_2$), the modified LeRoy criterion distance [24]. Therefore, the potential and its eigenvalues are solely determined by long-range interaction forces and the atomic spin-orbit fine-structure splitting, both of which are related to properties of the isolated atoms. The main idea here is to fit the theoretical eigenvalues of the 0_g^- state calculated by the model described below to the measured rovibrational binding energies to determine the correct long-range dipole-dipole potential constant C_3 and hence the radiative lifetime.

The experimental setup has previously been detailed [25]. Briefly, a ''dark spot'' vapor cell magneto-optical trap (MOT) prepares a sample of about 10^7 ^{39}K atoms with $>10^{11}$ atoms/cm^3 and at a temperature ~500 μK. The trapping laser beams are provided by a single-mode tunable ring Ti:sapphire laser with output power ~300 mW at 766.5 nm. A second such laser with output power up to ~1 W is used to induce the photoassociation. The absolute laser frequency is calibrated by uranium atomic lines as well as the potassium resonance lines. The laser frequency scan linearity is calibrated against two thermally stabilized étalons (free spectral ranges of 6.78 and 6.49 GHz) to <30 MHz. Trap fluorescence is monitored by a filtered photomultiplier tube, and a channeltron multiplier is used to detect ions generated by a multiphoton process described below.

The vibrational levels $v=5$ to 30 of the 0_g^- state are observed by photoassociation-induced trap loss [8,25]. Figure 1 presents a portion of our photoassociation spectrum of ^{39}K$_2$ observed below the $4s+4\,^2P_{3/2}$ asymptote. Three well-resolved vibrational series, 0_u^+, 1_g, and 0_g^- states, dissociat-
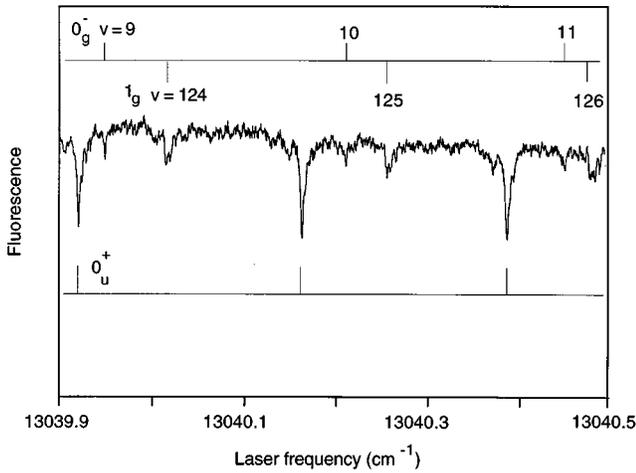
FIG. 1. A high-resolution portion of the photoassociation spectrum of $^{39}K_2$ observed below the $4\,^2S_{1/2}+4\,^2P_{3/2}$ asymptote (located at 13 042.876 cm^{-1}). Three well-resolved vibrational series, corresponding to the 0_u^+, 1_g, and 0_g^- states dissociating to the $4\,^2S_{1/2}+4\,^2P_{3/2}$ limit and showing some rotational structure, are assigned. The vibrational numberings for the 0_g^- and the 1_g states are counted from the bottom of their potential wells.

ing to the $4s+4\,^2P_{3/2}$ limit, are assigned as discussed in [25]. The lowest five vibrational levels $v=0$ to 4 are, however, not easily observed by such trap loss because the associated local kinetic energies for these levels are very small; when such levels undergo bound-free radiative decay (which conserves local kinetic energy by the Franck-Condon principle), the atoms cannot escape from the trap. Instead, low vibrational levels $v=0-9$ are observed by recording ion production through a two-color multiphoton ionization process as shown in Fig. 2. A specific rovibrational level (v,J) of the 0_g^- state is first populated by a photoassociation photon $h\nu_1$ via a free-bound transition. A second photon $h\nu_2$ excites the molecule to a specific long-range molecular state just below the highly excited $4s+5d$ atomic asymptote. The highly excited long-range molecule is then photoionized by $h\nu_1$ or $h\nu_2$. Figure 2 also shows the rotationally resolved spectrum of the
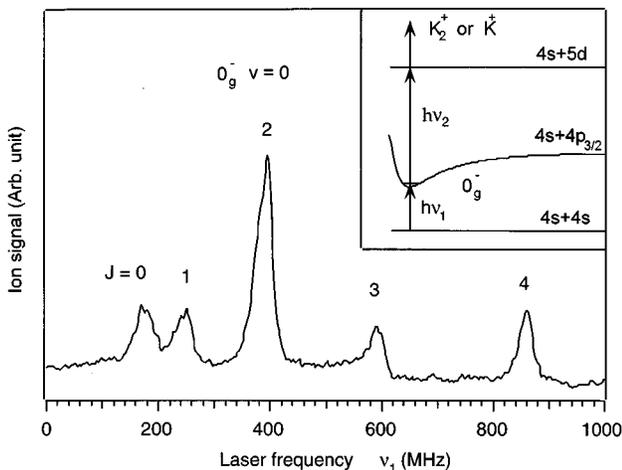
0_g^- $v=0$ level observed by monitoring the ion production while scanning ν_1. For these data, ν_2 is fixed at a broad double resonance peak with linewidth >1 GHz (and no rotational structure) due to autoionization [26]. Only rotational levels $J=0-4$ (resulting from the ground-state partial waves s, p, and d) are observed under our ultracold conditions (since higher partial waves do not significantly tunnel through the $l\geqslant3$ centrifugal barriers). High-resolution spectra of $v=0-9$ levels observed show that the $J=2$ peaks have the highest intensity due to the predominance of s-wave character in their absorption probability, similar to Na$_2$ [6]. For vibrational levels $v=5-30$ observed by trap loss (with a lower signal-to-noise ratio), only a single sharp peak for each vibrational level, assumed to be $J=2$, is clearly observed, as shown in Fig. 1. The vibrational binding energies are measured relative to the hyperfine-degeneracy-weighted center of the atomic state $4\,^2P_{3/2}$ ($F=0,1,2,3$). Since the initial free state involves $4s(F=1)+4s(F=1)$ collisions in a ''dark spot'' MOT, a hyperfine structure correction of 0.0100 cm^{-1} is added to each measured frequency difference between a molecular line and the atomic line [$4\,^2S_{1/2}$ ($F=1$) to $4\,^2P_{3/2}$ ($F=0,1,2$) transition]. Under our experimental conditions, a power shift of 21 MHz per 100 mW of probe laser power is typically observed in the trap loss spectra and corrected for in the analysis (probe laser powers of 50–500 mW were used). Due to the extremely high sensitivity of ion detection, very low probe laser powers (<1 mW) are used to generate the ion spectra (e.g., in Fig. 2), and no power shift is observed. As in the detailed line-shape analysis of Na photoassociation [6,27], the reference point of a photoassociation spectral line should be at the sharp blue edge of the line instead of the peak. In K, however, the difference between the line center and the blue edge (half-maximum intensity) is only ~7 MHz for the typical $J=2$ line, and negligible compared to the experimental uncertainty (estimated to be <60 MHz due to the calibration and the scan nonlinearity of the laser frequency). The 23 vibrational binding energies for $v=0-12$, 14–17, 19–22, 24, and 26 are used to determine the long-range constants C_3 and C_6 as described below. Missing levels are not unambiguously observed due to the overlap with 1_g and 0_u^+ levels.

At large internuclear distance ($R>1.7$ nm for K$_2$), the relativistic spin-orbit splitting $\Delta=57.706$ cm^{-1} is comparable to the long-range potential energy and the Hund's case (c) representation should be used. The adiabatic potential energies of the two 0_g^- states can be obtained by diagonalizing the appropriate 2×2 Hamiltonian in the Hund's case (a) basis with off-diagonal elements proportional to Δ [28–31]. The energy of the upper 0_g^- state (dissociating to $^2P_{3/2}$) is

FIG. 2. Very high-resolution rotational spectrum of the 0_g^- $v=0$ level observed by collecting ions produced via the multiphoton process schematically depicted in the inset.

$$E(0_g^-)=-\frac{1}{2}\left(\frac{\Delta}{3}-V_1-V_2\right)$$
$$+\frac{1}{2}\left[8\left(\frac{\Delta}{3}\right)^2+\left(V_1-V_2-\frac{\Delta}{3}\right)^2\right]^{1/2}, \quad (1)$$

and the wave function is a mixture of the two Hund's case (a) components: $|0_g^-,R\rangle=b_\Pi(R)|\Pi\rangle+b_\Sigma(R)|\Sigma\rangle$. In Eq. (1), $V_1=V(^3\Pi_{g\Omega=0^-})$ and $V_2=V(^3\Sigma_{g\Omega=0^-}^+)$ are the long-range potentials. Note that all energies (E, V_1, and V_2) are referred

to the spin-orbit degeneracy-weighted center of the $4p$ fine structure system. V_1 and V_2 can then be written as well-known (truncated) expansions in inverse powers of R:

$$V_{\Pi/\Sigma} = -f^{\Pi/\Sigma}\frac{C_3^{\Pi/\Sigma}}{R^3} - \frac{C_6^{\Pi/\Sigma}}{R^6} - \frac{C_8^{\Pi/\Sigma}}{R^8} \quad \text{for } R > R_{\text{LR-}m},$$
$$(2)$$

where $C_3^\Sigma = -2C_3^\Pi$ is the resonant dipole-dipole interaction constant, and $C_n^{\Pi/\Sigma}$ ($n = 6$ and 8) are the second-order dispersion constants. $f^{\Pi/\Sigma}$ represent the correction factors for retardation, which cannot be ignored at the current level of precision, and are given by the following equations [32,33]:

$$f^\Pi = \cos\left(\frac{R}{\lambda}\right) + \left(\frac{R}{\lambda}\right)\sin\left(\frac{R}{\lambda}\right) - \left(\frac{R}{\lambda}\right)^2\cos\left(\frac{R}{\lambda}\right), \quad (3)$$

$$f^\Sigma = \cos\left(\frac{R}{\lambda}\right) + \left(\frac{R}{\lambda}\right)\sin\left(\frac{R}{\lambda}\right), \quad (4)$$

where $\lambda_{4s-4p} = 2\pi\lambda$ is the transition wavelength. Retardation becomes important at large R when the interactions between the two atoms (which propagate at the speed of light) take a time comparable to the inverse of the transition frequency. Such an effect has already been observed in Na_2 [6] and Li_2 [3].

Given the potential-energy curve described by Eqs. (1)–(4), and the long-range constants, vibrational eigenvalues of the 0_g^- state are calculated by numerically solving the radial Schrödinger equation. The retardation effects described by Eqs. (3) and (4) increase the vibrational binding energies by 0.0044 cm^{-1} for $v = 0$, and 0.0020 cm^{-1} for $v = 30$. Similar to Na_2 [6], the electronic wave function of the 0_g^- state changes character from Σ to Π symmetry as a function of R. Because the $|0_g^-, R\rangle$ wave function defined below Eq. (1) has R-dependent coefficients [$b_\Pi(R)$ and $b_\Sigma(R)$], the 0_g^- state can be corrected by the diagonal nonadiabatic term $\langle 0_g^-, R|T^N|0_g^-, R\rangle$, where $T^N \sim d^2/dR^2$. The operator does not act on the Π and Σ wave functions but on the R-dependent coefficients. This correction is calculated to slightly decrease the binding energies by 0.000 95 cm^{-1} for $v = 0$, and 0.000 05 cm^{-1} for $v = 30$.

The rotational energy of the 0_g^- state can be estimated by rewriting the Movre-Pichler Hamiltonian [29] in terms of linear superposition of atomic states. In such an expansion one can clearly show that $J = l + j$, where $j = j_a + j_b$ and j_a and j_b are the internal angular momenta of the two atoms. The rotational Hamiltonian is $l^2/2\mu R^2$, and thus

$$E^{\text{rot}}(R) = \left(\frac{\hbar^2}{2\mu R^2}\right)[J^2 - 2Jj + j^2]$$

$$= \left(\frac{\hbar^2}{2\mu R^2}\right)[J(J+1) - 2\Omega^2 + j_x^2 + j_y^2 + \Omega^2], \quad (5)$$

which for $\Omega = 0$ states is proportional to $J(J+1) + \langle j(j+1)\rangle$. For 0_g^- states, $j = 0$ or 2 where $j = 0$ correlates to $4S_{1/2} + 4P_{1/2}$, and $j = 2$ correlates to $4S_{1/2} + 4P_{3/2}$. The $\langle j(j+1)\rangle$ term in Eq. (5) is the correction for the rotational energy of the $J = 0$ total angular momentum state, and physically accounts for the fact that the atoms have internal

structure. For the upper 0_g^- state this will asymptotically yield six units of mechanical rotational energy. This correction term contributes 0.0059 cm^{-1} for $v = 0$ and 0.0011 cm^{-1} for $v = 30$, and has an opposite sign to that of the retardation corrections. Since the K atom has very small hyperfine splittings (462 MHz for $4s$ and ~30 MHz for $4p$), the molecular hyperfine splittings associated with the 0_g^- state are negligible for the observed vibrational levels at the current experimental precision.

The calculated rovibrational eigenvalues are then least-squares fitted to the experimental binding energies for $J = 2$. During the fitting, only the long-range constants C_3 and C_6 are varied around the theoretical values given in Ref. [34] with the ratios of C_3^Π/C_3^Σ and the C_6^Π/C_6^Σ unchanged. Due to their small contributions to the long-range potentials, the fitting is insensitive to changing the C_8 constants, and thus they are fixed at the theoretical values. The fit returns the experimentally determined long-range constants $C_3^\Pi = -C_3^\Sigma/2 = -5.456(9)$ zJ nm$^3 = -8.445(14)$ a.u. Our values of C_3 and C_6 are 2.54% smaller and 3.0% larger than the latest theoretical ones by Marinescu and Dalgarno [34], respectively. We notice that all three correction terms (for the effects of retardation, nonadiabatic behavior, and nonzero angular momentum) contribute more to the low vibrational levels than to the higher ones, and mainly cause changes in C_6 during the fitting (a −15% change in C_6 from the theoretical value is needed for the best fit if these corrections are not included). The long-range dipole-dipole constant C_3, however, is not very sensitive to these corrections because it is largely determined by the binding energies of the higher vibrational levels, which are less influenced by these corrections. The best fit has a statistical one σ standard deviation of 0.0013 cm^{-1} between the experimental and the calculated binding energies, $E_{\text{expt}}(v, J = 2) - E_{\text{calc}}(v, J = 2)$, over the 23 vibrational levels. On the other hand, the uncertainty for the calculated eigenvalues is estimated to be ~0.001 cm^{-1} mainly from the effects of hyperfine interactions and limitations of the theoretical model. The overall uncertainties for the resulting constants are determined by projecting the rms sum (0.0016 cm^{-1}) of these two independent errors on the fitting. As an independent confirmation [31] of the above results, we also fit the calculated long-range potential of the 1_g ($1\,^1\Pi_g$ at short R) state to the long-range portion (26−30.6 bohr) of the experimentally determined Rydberg-Klein-Rees (RKR) potential of the $1\,^1\Pi_g$ state [35]. This fit
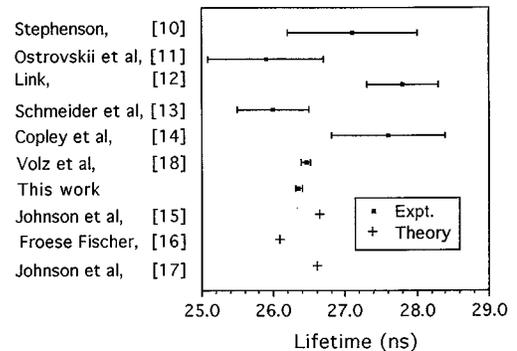
FIG. 3. Comparisons of the experimental and theoretical values of the radiative lifetime of the K $4\,^2P_{3/2}$ state.

gives a value of C_3 that agrees within one standard deviation.

The radiative lifetimes of the K $4\,^2P_{3/2}$ and $4\,^2P_{1/2}$ states are then derived from the square of the dipole matrix element $(-C_3^{\Pi})$ to be $\tau(4\,^2P_{3/2})=26.34(5)$ ns and $\tau(4\,^2P_{1/2})=26.69(5)$ ns [36]. The quoted uncertainty is one standard deviation. Figure 3 compares our result for $4\,^2P_{3/2}$ with previous experimental and theoretical determinations. Our present measurement and the recent fast-beam measurement $[\tau=26.45(7)$ ns$]$ [18] agree within their combined (and similar) uncertainties. These two most recent measurements are consistent with previous experiments, due to the relatively large uncertainties of the latter. However, the recent results agree only marginally with the theoretical values.

In conclusion, we have observed the ''pure long-range'' 0_g^- state of $^{39}K_2$ with rotational resolution for vibrational levels $v=0-30$ by photoassociative spectroscopy of ultracold ^{39}K atoms. The measured binding energies are used to determine precisely the dipole matrix element and the radiative lifetime of the K $4p$ state with an accuracy of 0.2%. The current measurement agrees well with the recent fast-beam experiment, significantly improving the value of the radiative lifetime of the K $4p$ state. In order to best fit the experimental data, the theoretical model has to take into account various corrections such as higher-order dispersion forces (C_6 and C_8), retardation, nonadiabatic coupling, and nonzero angular momentum.

[1] C. S. Wood *et al.*, in *Proceedings of the 14th International Conference on Atomic Physics, Boulder, CO, 1994*, Abstracts of Contributed Papers (University of Colorado, Boulder, 1994), p. 1D-1.

[2] W. I. McAlexander *et al.*, Phys. Rev. A **51**, R871 (1995).

[3] W. I. McAlexander, E. R. I. Abraham, and R. G. Hulet, Phys. Rev. A **54**, R5 (1996).

[4] U. Volz *et al.*, Phys. Rev. Lett. **76**, 2862 (1996).

[5] C. W. Oates, K. R. Vogel, and J. L. Hall, Phys. Rev. Lett. **76**, 2866 (1996).

[6] K. M. Jones *et al.*, Europhys. Lett. **35**, 85 (1996).

[7] H. R. Thorsheim, J. Weiner, and P. S. Julienne, Phys. Rev. Lett. **58**, 2420 (1987).

[8] P. D. Lett, P. S. Julienne, and W. D. Phillips, Annu. Rev. Phys. Chem. **46**, 423 (1995).

[9] E. Tiemann, H. Knockel, and H. Richling, Z. Phys. D **37**, 323 (1996).

[10] G. Stephenson, Proc. Phys. Soc. London, Sec. A **64**, 458 (1951).

[11] Y. I. Ostrovskii and N. P. Penkin, Opt. Spektrosk. **12**, 669 (1962) [Opt. Spectrosc. **12**, 379 (1962)].

[12] J. K. Link, J. Opt. Soc. Am. **56**, 1195 (1966).

[13] R. W. Schmeider, A. Lurio, and W. Happer, Phys. Rev. **173**, 76 (1968).

[14] G. Copley and L. Krause, Can. J. Phys. **47**, 533 (1969).

[15] W. R. Johnson, M. Idrees, and J. Sapirstein, Phys. Rev. A **35**, 3218 (1987).

[16] C. Froese Fischer, Nucl. Instrum. Methods Phys. Res. Sect. B **31**, 265 (1988).

[17] W. R. Johnson, Z. W. Liu, and J. Sapirstein, At. Data Nucl. Data Tables **64**, 279 (1996).

[18] U. Volz and H. Schmoranzer, Phys. Scr. **65**, 48 (1996).

[19] W. C. Stwalley, Y.-H. Uang, and G. Pichler, Phys. Rev. Lett. **41**, 1164 (1978).

[20] D. Kleppner, Phys. Today **48**(7), 11 (1995).

[21] R. A. Cline, J. D. Miller, and D. J. Heinzen, Phys. Rev. Lett. **73**, 632 (1994).

[22] L. P. Ratliff *et al.*, J. Chem. Phys. **101**, 2638 (1994).

[23] H. Wang, P. L. Gould, and W. C. Stwalley, Z. Phys. D **36**, 317 (1996).

[24] B. Ji, C. C. Tsai, and W. C. Stwalley, Chem. Phys. Lett. **236**, 242 (1995); also see R. J. Le Roy, in *Molecular Spectroscopy*, edited by R. F. Barrow, D. A. Long, and D. J. Millen (Chemical Society, London, 1973), Vol. 1, p. 113.

[25] H. Wang, P. L. Gould, and W. C. Stwalley, Phys. Rev. A **53**, R1216 (1996).

[26] H. Wang, X. T. Wang, P. L. Gould, and W. C. Stwalley (unpublished).

[27] R. Napolitano *et al.*, Phys. Rev. Lett. **73**, 1352 (1994).

[28] E. I. Dashevskaya, A. I. Voronin, and E. E. Nikitin, Can. J. Phys. **47**, 1237 (1969).

[29] M. Movre and G. Pichler, J. Phys. B **10**, 2631 (1977).

[30] S. Magnier and Ph. Millie, Phys. Rev. A **54**, 204 (1996).

[31] H. Wang, P. L. Gould, and W. C. Stwalley, J. Chem. Phys. (to be published).

[32] R. McLone and E. Power, Mathematika **11**, 91 (1964).

[33] W. J. Meath, J. Chem. Phys. **48**, 227 (1968).

[34] M. Marinescu and A. Dalgarno, Phys. Rev. A **52**, 311 (1995).

[35] A. J. Ross *et al.*, Indian J. Phys. B **60**, 309 (1986). In this work, the molecular constants were derived without taking into account the Λ^2 term in the rotational energy $E=B[J(J+1)-\Lambda^2]$. The RKR potential is, therefore, corrected by a term of $\hbar^2/2\mu R^2$.

[36] The prediction [Y.-K. Kim (private communication) and Refs. [15–17]] that the matrix elements for the two components differ slightly due to relativistic corrections $|d_{3/2}|^2/|d_{1/2}|^2=0.9993(1)$, does not affect our spectroscopic analysis or lifetime determinations at the current level of uncertainty. Differences between the $P_{3/2}$ and $P_{1/2}$ lifetimes are due solely to differences in λ [C. Corliss and J. Sugar, J. Phys. Chem. Ref. Data **8**, 1109 (1979)].